

## Fabrication and Characteristics of Cast Aluminium-Mineral Particles Composite

Marcin Kargul<sup>1</sup>, Joanna Borowiecka-Jamrozek<sup>1\*</sup>

<sup>1</sup> Faculty of Mechatronics and Mechanical Engineering, Kielce University of Technology, al. Tysiąclecia Państwa Polskiego 7, 25-314 Kielce, Poland

\* Corresponding author's e-mails: jamrozek@tu.kielce.pl

### ABSTRACT

The paper presents the results of research on the production of cast composites based on aluminum alloys with a mineral filler with a porous structure. AlSi12 silumin and AlSi12 silumin with the addition of 3% magnesium (AlSi12-Mg3) were used as the matrix material, while particles of natural zeolite, expanded perlite and expanded clay with a size of 4 to 6 mm were used as the mineral filler. In order to increase the efficiency of the production process, the mineral particles have been covered with a sodium silicon solution with the addition of silicon powder. The coated particles were then heated at 400 °C for 1 hour to remove moisture from them. The prepared mineral particles were then placed inside a casting mold and flooded with liquid alloy at a temperature of 790 °C. The obtained composites were subjected to macroscopic observations and analysis using computed tomography (CT). Phase analysis was also performed to determine the phase composition of the obtained composites. In order to determine the mechanical and physical properties, the obtained composites were subjected to compressive strength tests and density measurements. As a result of the research, it was found that the use of the AlSi12-Mg3 alloy and coating in the form of a solution of sodium silicate and silicon powder allows for the most effective production of composites. The low density of the produced composites, combined with their favorable structure and strength properties, suggest the possibility of use as light products transferring compressive stresses, as well as energy-absorbing products.

**Keywords:** aluminum alloys, zeolite, expanded perlite, expanded clay.

### INTRODUCTION

Composite porous materials have a significant amount of empty spaces in their structure, which makes them low density. These composites are called metallic foams. Depending on the type of pores, metallic foams can be divided into three groups: metallic foams with open pores, metallic foams with closed pores and metallic foams filled with porous particles of the second phase [1]. Composite materials filled with porous particles of the second phase are called syntactic foams (MMSF - Metal Matrix Syntactic Foams) in the professional literature [2]. Syntactic foams are unique composite materials with a metal matrix filled with second-phase particles, most often in the form of hollow ceramic balls or porous particles of expanded perlite and other minerals.

Syntactic foams are characterized by high energy absorption capacity and relatively high strength, which, combined with very low density, makes syntactic foams an attractive engineering material. High absorption capacity makes syntactic foams suitable for use in the automotive and defense industries [3]. However, the low density combined with the relatively high strength of syntactic foams allows them to be used in the transport industry (weight reduction results in lower fuel consumption). Light metals are most often used as matrix materials for the production of syntactic foams. Aluminum is the most commonly used matrix material for syntactic foams due to its low density, good castability, good machinability and relatively low price. In addition, aluminum alloys can be additionally strengthened by heat treatment [4, 5]. Another metal used for

the production of syntactic foams is magnesium. Like aluminum, it is characterized by low density, but has a higher price and lower machinability. Magnesium alloys are characterized by high reactivity and therefore it is difficult to produce syntactic foams using the casting method [6]. In addition to the above-mentioned metals, zinc [7, 8], titanium and iron alloys are also used to produce syntactic foams [9,10]. Low density of syntactic foams is achieved by introducing hollow spheres or porous particles into the metal matrix. Hollow particles are usually introduced in the form of balls made of aluminum oxide or glass [11, 12]. In the professional literature you can also find information about hollow spheres made of steel [13]. In the case of porous particles, the most commonly used are expanded perlite [14], expanded glass [15] or expanded clay [16]. Syntactic foams are most often produced by stir casting or pressure infiltration, less frequently by gravity casting and powder metallurgy [17, 18]. In addition to the advantages of syntactic foams, there are also their disadvantages. The engineering materials used to produce hollow particles are highly expensive. For this reason, cheap, available mineral materials such as expanded perlite are increasingly used [19]. The use of ceramic particles reduces the strength properties of porous composites. Moreover, the use of mineral particles complicates the process of making syntactic foams by gravity casting. Research is also being carried out on the production of coatings for the introduced particles in order to influence their behavior during contact with the liquid melt. Literature data shows that coatings can be obtained by chemical or physical vapor deposition or electrodeless deposition of metals. These techniques significantly increase production costs and require the use of chemicals that may negatively impact the environment [20]. As part of this work, research was carried out on the production of composites based on aluminum alloys with a filler in the form of porous mineral particles containing a coating that improves wettability. Light mineral materials were selected as the filler particles in the form of zeolite, expanded perlite and expanded clay. The

work also analyzed the possibility of enriching commercial aluminum alloys with additional alloying elements to improve the properties of the produced composites.

## RESEARCH METHODOLOGY

The material for the composite matrix was selected from commercially available foundry aluminum alloys containing silicon (silumins). Silumins have very good casting properties and high abrasion resistance. Silumins may contain various alloy additives that have a beneficial effect on the mechanical properties and castability of the alloys [21]. The criteria for selecting alloys in the presented work were their casting and mechanical properties, as well as the tests carried out on the production of composites. The work also analyzed the possibility of enriching commercial aluminum alloys with additional alloying elements to improve the properties of the manufactured composites. For this purpose, 3% Mg by weight was added to the AlSi12 alloy (alloy referred to as AlSi12-Mg3). Table 1 presents the chemical composition of the tested composite matrix materials. Light mineral materials were selected as the filler particles in the form of zeolite, expanded perlite and expanded clay.

Zeolite belongs to the group of aluminosilicates minerals. Its chemical composition includes hydrated aluminosilicates, most often sodium and calcium, less frequently barium, strontium, potassium, magnesium and manganese. The density of zeolites ranges from 1.8 to 2.3 g/cm<sup>3</sup>, while the hardness, depending on the chemical composition, ranges from 3 to 5.5 on the Mohs scale. Thanks to unique properties such as: negative charge of the crystal lattice, crystalline structure, thermal and hydrothermal stability, uniform micropore size, easy exchange of off-lattice cations and others, they can be used in various fields such as: ion exchange, catalysis, water and exhaust gas purification or processing. crude oil [22].

Perlite is a naturally occurring rock of volcanic origin that contains several percent water.

**Table 1.** Aluminum alloys used as the matrix of composites

Materials	Chemical composition/purity, % by mass
AlSi12	11,39 Si; 0,39 Fe; 0,02 Mn, Al balanced
AlSi12-Mg3	AlSi12 + 3% Mg

Expanded perlite is produced from perlite. The production process includes heating perlite rock at a temperature of 850–1000 °C. As a result of heating, the rock softens and the water escaping from it causes the material to expand. As a result, the density of perlite rock decreases from 1.0–1.2 g/cm<sup>3</sup> to 0.03–0.25 g/cm<sup>3</sup>. Perlite consists mainly of oxides of silicon, aluminum, potassium, sodium, iron, calcium and magnesium [23].

Expanded clay is a light aggregate fired from clayey clay at a temperature of approximately 1150 °C. It is produced from swelling clays. Expanded clay has a porous internal structure surrounded by a hard ceramic shell on the outside. Depending on the fraction obtained, the density of expanded clay varies from 0.23 to 0.58 g/cm<sup>3</sup>. The obtained aggregate is a non-flammable, chemically inert material, resistant to water and many organic substances. It has good thermal insulation parameters [24]. The shapes of the mineral particles used in the experiments are shown in Figure 1.

Based on the tests, the particle size of the zeolite, expanded perlite and expanded clay filler was selected to produce composites with the fewest casting defects. The paper presents test results for composites containing fillers with a particle diameter of 4–6 mm. Composites were produced using uncoated mineral particles and with an additional coating of another material. Silicon powder was used as the covering material. The silicon powder was applied to the ceramic particles by mechanical or manual mixing in the presence of an additional liquid in the form of an aqueous solution of sodium silicate. The addition of sodium silicate served as a substance that allowed the filler particles to be permanently covered with another material. The following mass proportions of ingredients were used: 82% filler, 9% powdered substance and 9% aqueous solution of sodium silicate. After applying the coating, the filler

particles were then heated for 1 hour at 400 °C to remove the water they contained. In the next stage, a sand casting mold was produced. The preliminary tests carried out enabled the selection of the mold geometry and parameters of the composite manufacturing process. The molding sand used consisted of 92% fine quartz foundry sand and 8% foundry bentonite. The mass was prepared with the addition of 5% water. A channel was designed in the casting mold, inside which particles of mineral filler were placed. The designed shape of the channel was aimed at assessing the ability of the liquid alloy to fill the space between the filler particles. Due to the presence of filler particles and their effect on reducing the speed of filling the mold with the liquid melt, it was decided to use a relatively large cross-section of the pouring system. The low density of filler particles compared to the density of the aluminum alloy forced the use of a bottom gating system. The advantage of using this type of pouring system is the smooth filling of the mold, which translates into a low risk of damaging the mold cavity during pouring. In order to keep the filler particles inside the channel during pouring, an overflow with a diameter smaller than the filler fraction was used. The composite manufacturing process included preparing the molding sand using a circular mixer, followed by making a casting mold at the molding station using models imitating the shape of the manufactured composite and elements of the gating system. The casting mold consisted of two parts. Punctures were made in the upper part to increase the permeability of the form. For molding work, a pneumatic rammer operating at a pressure of 5 bar and manual casting tools were used. The manufactured molds were dried at ambient temperature for 72 h, after which the internal channel was completely filled with the prepared filler particles. The temperature

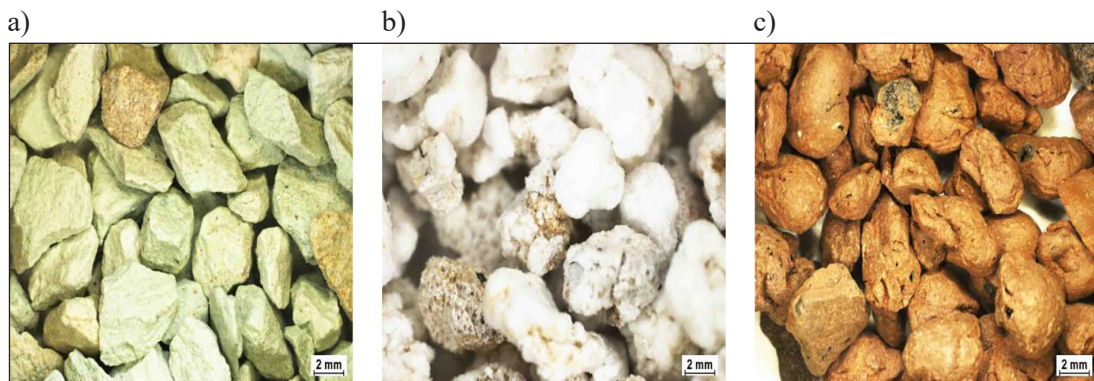


**Figure 1.** Shapes of the mineral particles: (a) zeolite, (b) expanded perlite, (c) expanded clay

of pouring the aluminum alloy into the mold was 790 °C. Figure 2 shows the geometry of the casting mold used to produce the composites.

The manufactured composites were subjected to structural observations to determine the degree of filling of the channel inside the mold and to assess the presence of casting defects. Observations were carried out using optical microscopy (Nikon AZ100 Optical Macroscope and Nikon MA200 Optical Microscope, equipped with the NIS 4.2 image analysis system). Measurements of the length of the filled part of the canal were carried out using an electronic caliper. The results are presented in the form of an arithmetic mean for the length of the part of the channel filled with aluminum alloy, measured on the side edges of the sample.

Based on casting tests carried out for various combinations of matrix material/mineral filler/covering of filler particles, the component materials used to create a composite with a favorable structure and the lowest number of casting defects were selected. Selected composites were further analyzed using a Nikon Microfocus computed tomography system with a 225 kV X-ray source. The tested samples were also subjected to phase analysis using the XRD method in order to determine the phase composition of the manufactured composites and to learn about the chemical reactions occurring during the manufacturing process. Phase analysis was performed on a Bruker D8 Discover device equipped with a Co-K $\alpha$  anode. The next stage of the research included the analysis of the mechanical properties of selected composites. A static compression test was carried out using the ZD-100 universal testing machine with a load of up to 1000 kN. Cubic samples with dimensions of 18×18×18 mm were used for strength tests. The strain rate was 2 mm/min. Moreover, the manufactured composites were subjected to density tests.

## ANALYSIS OF THE RESULTS

### Macro-structural investigations

Figure 3 shows an example macrostructure for aluminum alloy/zeolite composites. The presence of filler particle coverage and the aluminum alloy used significantly affect the number of casting defects in the produced composite. Table 2 collects the results of measuring the length of the channel part that was filled with aluminum alloy. The results for the variant in which the zeolite particles were not coated with silicon are shown in Figure 3a. Zeolite particles clearly impede the flow of liquid alloy into the channel in which they are located. In this case, the average length of the channel filled with aluminum alloy was only 15.2 mm. Figure 3b shows the structure observed in the case where the filler particles were used with an additional Si coating. In this variant, the aluminum alloy filled the spaces between the particles in the mold cavity to a much greater extent. The positive effect of the coating on mineral particles was also observed by other researchers [20, 25]. The average length of the filled portions of the channel was nearly 6 times greater compared to samples with uncoated zeolite particles. When Si-coated zeolite particles were flooded with AlSi12-Mg3 alloy (Figure 3c), complete filling of the channel spaces occurred. The obtained results confirmed the literature information about the beneficial effect of the addition of magnesium on the castability of aluminum alloys, which was the premise for producing an alloy with the addition of magnesium. Applied coating of the zeolite filler particles with silicon powder influenced the ability of the liquid alloy to penetrate the space between the particles. The use of a coating in the form of silicon powder has a positive effect on the viscosity and surface phenomena of the liquid aluminum alloy in contact with the surface of the filler particles.

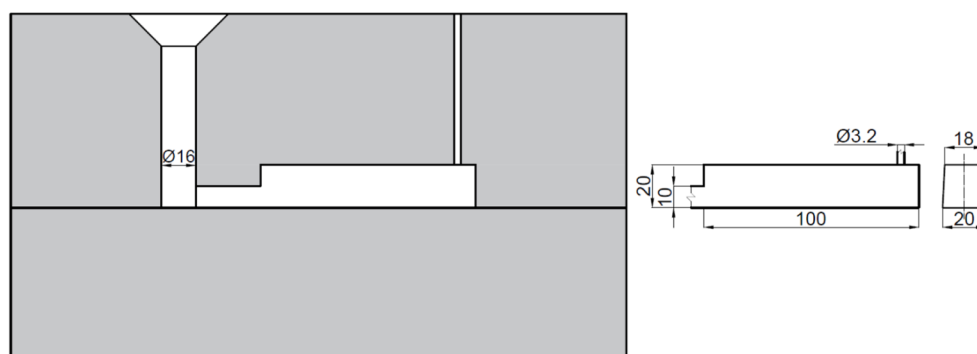


**Figure 2.** Geometry of the sand casting mold used

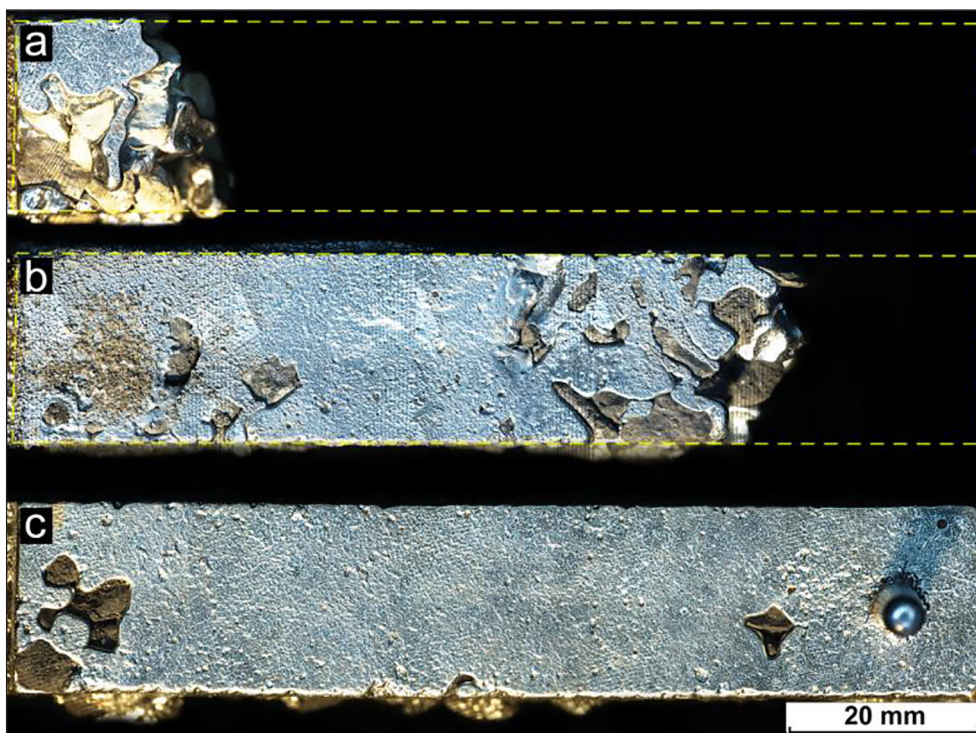


**Figure 3.** Representative structure of composites prepared by pouring Al alloy into zeolite particles. Variant: (a) AlSi12 alloy, particles without coating; (b) AlSi12 alloy, Si coated particles; (c) AlSi12-Mg3 alloy, Si coated particles

**Table 2.** Aluminum alloys used as the matrix of composites

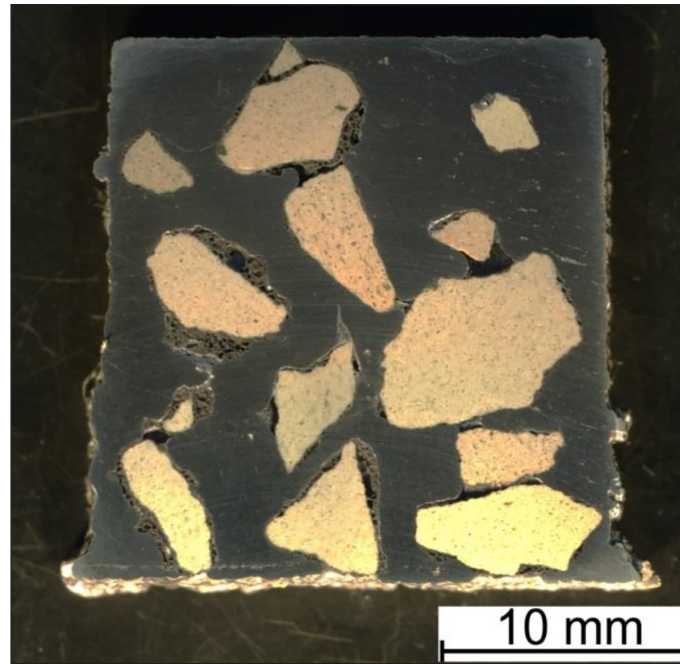
Variant	Length of the filled part of the canal, mm			
	1	2	3	Average
AlSi12, particles without coating	12.1	19.6	14.0	15.2
AlSi12, Si-coated particles	87.4	100.0	82.7	90.0
AlSi12-Mg3, Si-coated particles	100.0	100.0	100.0	100.0

Figure 4 shows the structure observed in the cross-section of the AlSi12-Mg3/zeolite composite produced using silicon-coated filler particles. Space between the filler particles is well filled with the alloy, with small pores located at the border of the composite components. Microscopic observations indicate that there was no gravitational lifting of filler particles despite their lower density compared to the liquid AlSi12-Mg3 alloy. This phenomenon may be due to the fact that the filler particles occupied the entire volume of the channel in the casting mold. The obtained result indicates the isotropy of the functional properties of the produced composites on a macroscopic scale.

Figure 5 presents a macroscopic image of AlSi12-Mg3/expanded perlite composites produced using uncoated filler particles and silicon-coated particles. In both variants the entire length of the

channel was filled in the casting mold. These results indicate a beneficial effect of expanded perlite particles on the phenomena occurring in contact with the liquid AlSi12-Mg3 alloy. Further observations carried out on cross-sections of AlSi12-Mg3/expanded perlite composite samples (Figure 6) confirmed the favorable behavior of expanded perlite during the pouring process. Samples obtained both without particle coating and with Si coating were characterized by the lack of significant defects in the cross-section of the samples, and the distribution of filler particles was even.

Figure 7 shows an image of AlSi12-Mg3/expanded clay composites produced for the variant with uncoated filler particles and when the filler particles were covered with silicon. In this case, the entire length of the channel was also filled in the casting mold for samples from both analyzed variants. These



**Figure 4.** Cross-section of composites made using zeolite particle filler with Si coating

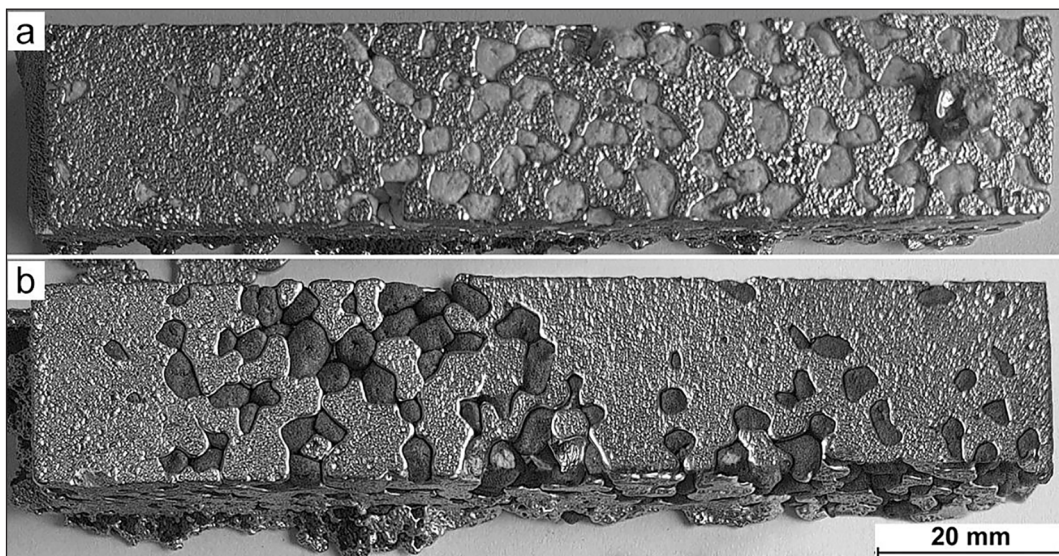


**Figure 5.** Representative structure of AlSi12-Mg3/expanded perlite composites produced using filler particles: (a) without coating, (b) with Si coating

results confirm that expanded clay behaves favorably in contact with the liquid AlSi12-Mg3 alloy and for the applied process parameters it is not necessary to use a coating that affects surface phenomena at the filler particle/liquid alloy interface. A macroscopic image of the cross-section of AlSi12-Mg3/expanded clay samples (Figure 8) showed that the analyzed composites were characterized by a favorable structure, without major casting defects, and the filler particles were evenly distributed in the matrix.

### Computed tomography analysis

Figure 9 shows the result of a three-dimensional analysis of the AlSi12-Mg3/zeolite composite with silicon-coated filler particles, carried out using a computed tomography system. A uniform distribution of mineral particles in the metal matrix can be observed. The three-dimensional images of the composite showed small pores, located mainly at the interface between the matrix and the filler particles.

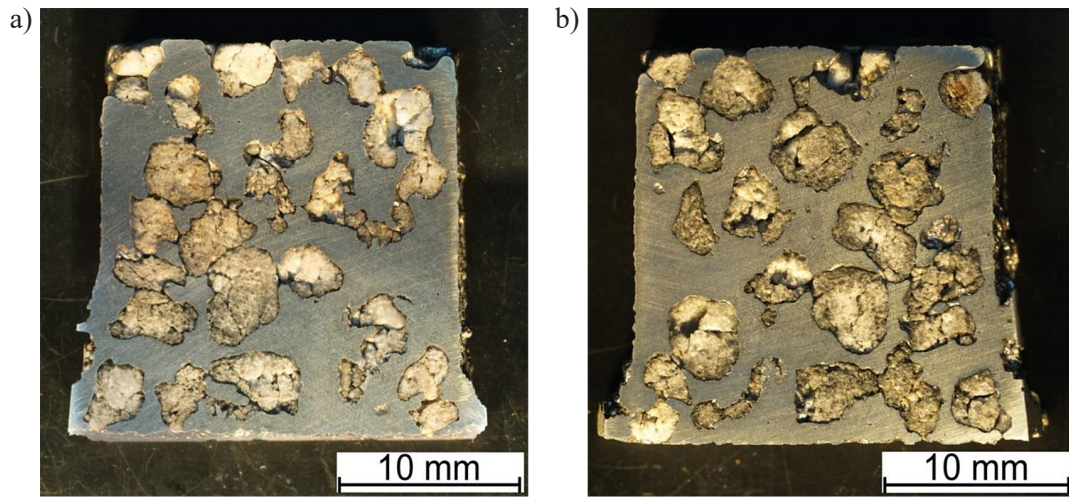


**Figure 6.** Cross-section of AlSi12-Mg3/expanded perlite composites produced using filler particles: (a) without coating, (b) with Si coating

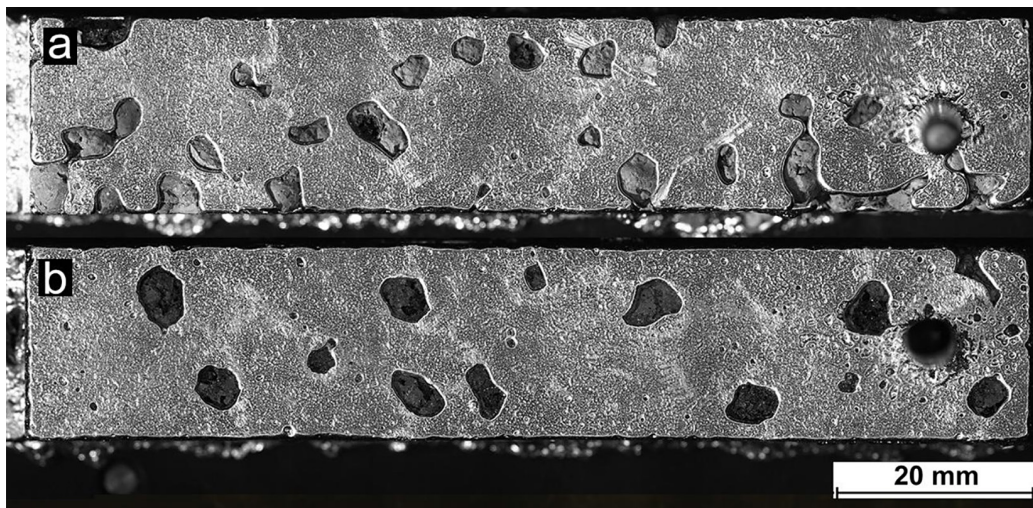


**Figure 7.** Representative structure of composites made using a filler in the form of expanded clay particles: (a) particles without coating, (b) particles with Si coating

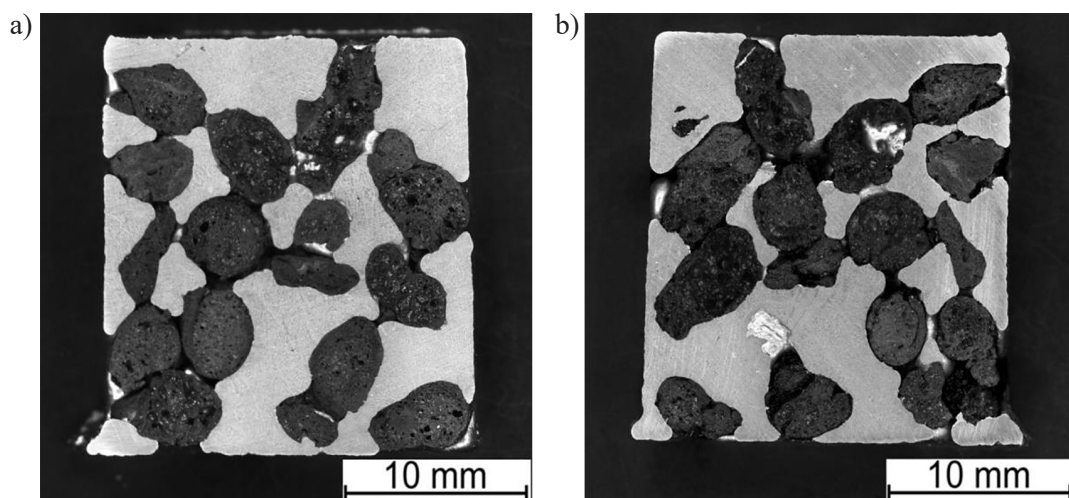


**Figure 8.** Cross-section of composites made using a filler in the form of expanded clay particles: (a) particles without coating, (b) particles with Si coating

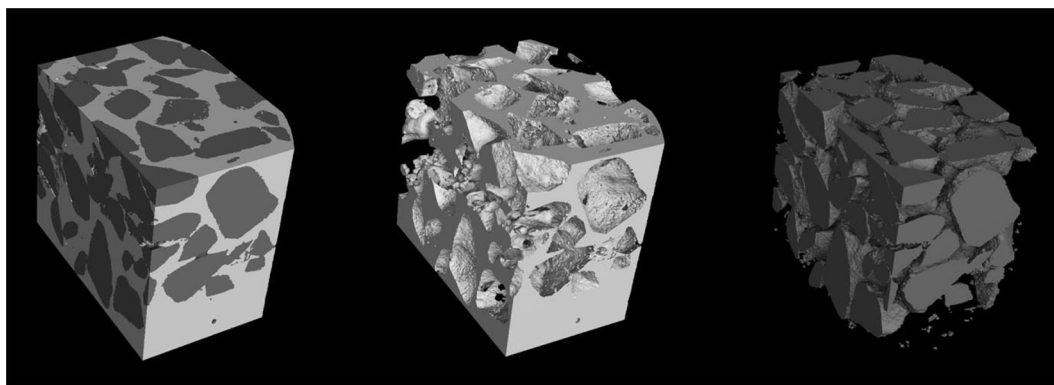


**Figure 9.** Three-dimensional tomographic scan of a sample made of AlSi12-Mg3/zeolite composite with silicon-coated filler particles

Figure 10 presents the result of the tomographic analysis for the AlSi12-Mg3/expanded perlite sample, both for the variant with uncoated filler particles and with the filler covered with silicon. In both analyzed cases, even distribution of filler particles and no major internal defects were observed. The result for the AlSi12-Mg3/expanded clay composite (Figure 11) also confirmed the favorable structure of the obtained product, both for the variant with uncoated filler particles and with the filler covered with silicon. In both analyzed cases, an even distribution of filler particles and small pores on the boundary between the matrix and filler particles, which were located mainly in the surface part of the composite.

### Phase composition analysis

Figures 12–15 show the results of the phase composition analysis using the XRD method for the component materials of the composites presented in this work (AlSi12-Mg3 alloy, zeolite,

expanded perlite, expanded clay). The results for the AlSi12-Mg3 alloy showed that its composition includes the following phases: Al, Si, Mg<sub>2</sub>Si and Fe<sub>4</sub>Al<sub>17.5</sub>Si<sub>1.5</sub>. In the case of zeolite, a complex phase composition was observed, in which multi-component compounds were present, such as: clinoptilolite-Ca(KNa<sub>2</sub>Ca<sub>2</sub>(Si<sub>29</sub>Al<sub>7</sub>)O<sub>72</sub>·24H<sub>2</sub>O), clinoptiloliteNa((Na,K,Ca)<sub>6</sub>(Si,Al)<sub>36</sub>O<sub>72</sub>·20H<sub>2</sub>O), albite- Ca((Na,Ca)(Si,Al)<sub>4</sub>O<sub>8</sub>), quartz (SiO<sub>2</sub>).

The diffractogram for expanded perlite indicated the amorphous structure of this mineral, which is confirmed by literature data stating that expanded perlite is silica particles with an amorphous structure (SiO<sub>2</sub>). Expanded clay is composed of the following phases: anorthite (CaAl<sub>2</sub>Si<sub>2</sub>O<sub>8</sub>), calcium-magnesium-silicon oxide (Ca<sub>0.8</sub>Mg<sub>1.2</sub>Si<sub>2</sub>O<sub>6</sub>), quartz (SiO<sub>2</sub>). Figure 16 shows the X-ray diffractogram for a sample of the AlSi12-Mg3/zeolite composite with silicon-coated filler particles. Contact of liquid aluminum alloy with silicon-coated zeolite particles did not lead

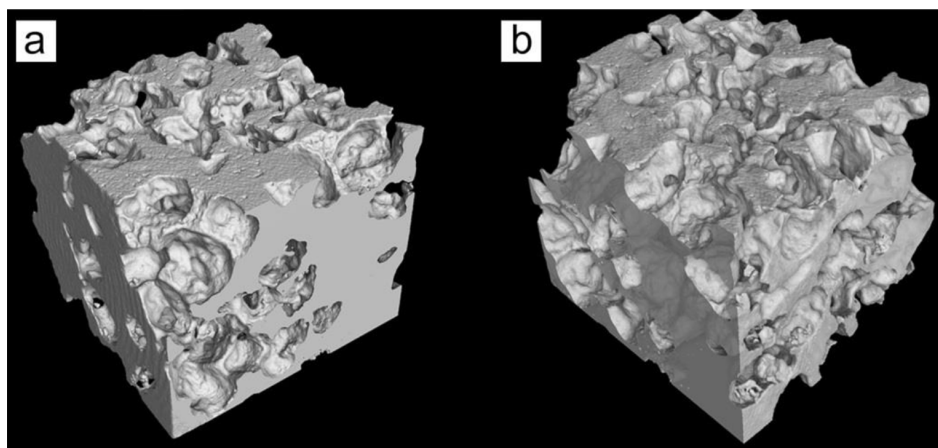


**Figure 10.** Three-dimensional tomographic scan for a sample of the AlSi12-Mg3/expanded perlite composite: (a) sample with uncoated filler particles; (b) sample with silicon-coated filler particles

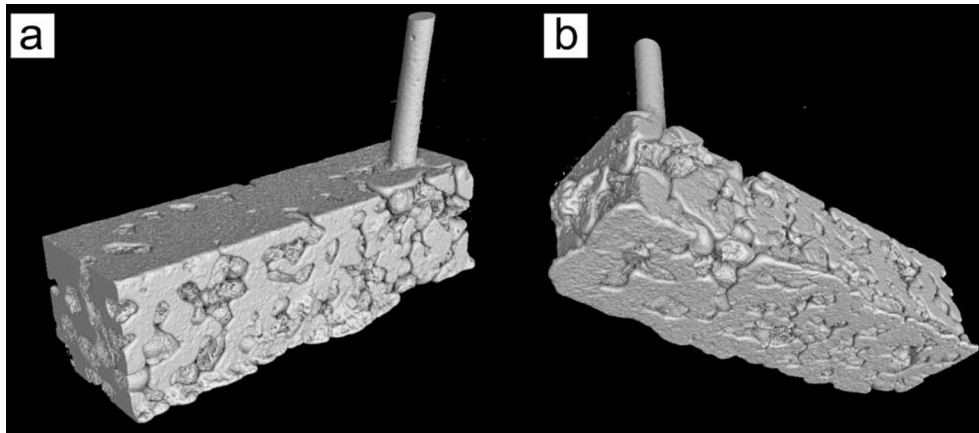


**Figure 11.** Three-dimensional tomographic scan for a sample of the AlSi12-Mg3/expanded clay composite: (a) sample with uncovered filler particles; (b) sample with silicon-coated filler particles

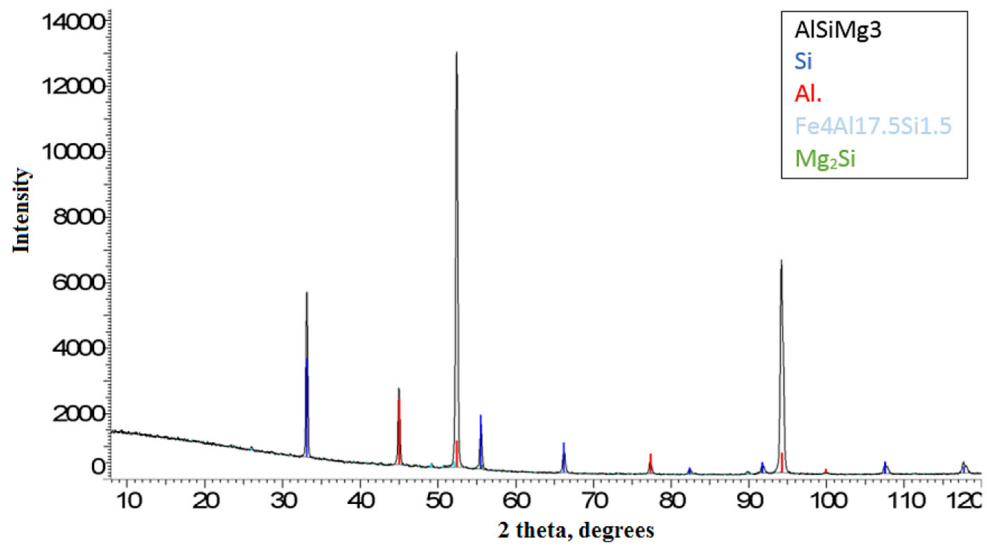


**Figure 12.** X-ray diffractogram pattern for a sample from the AlSi12-Mg3 alloy

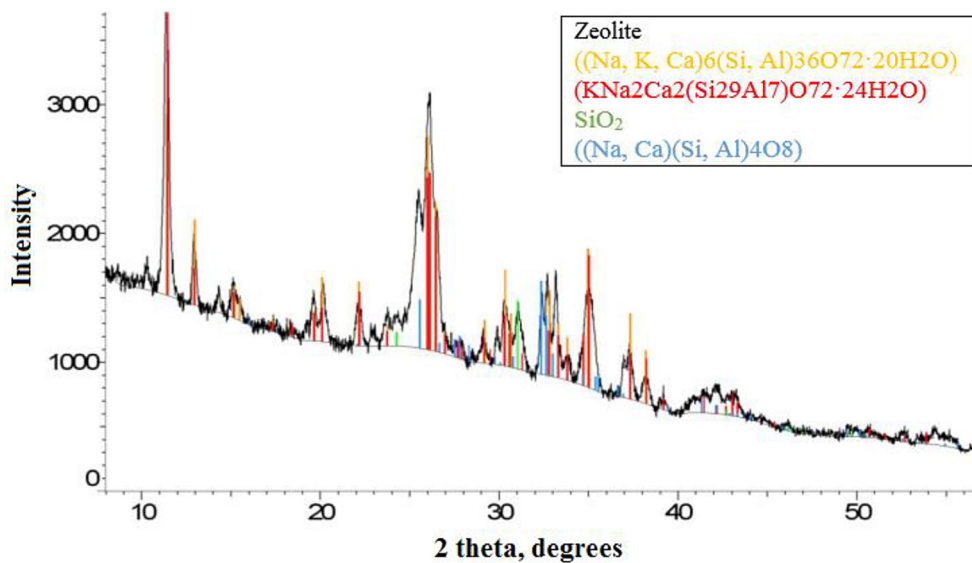


**Figure 13.** X-ray diffraction pattern for a sample made of zeolite particles

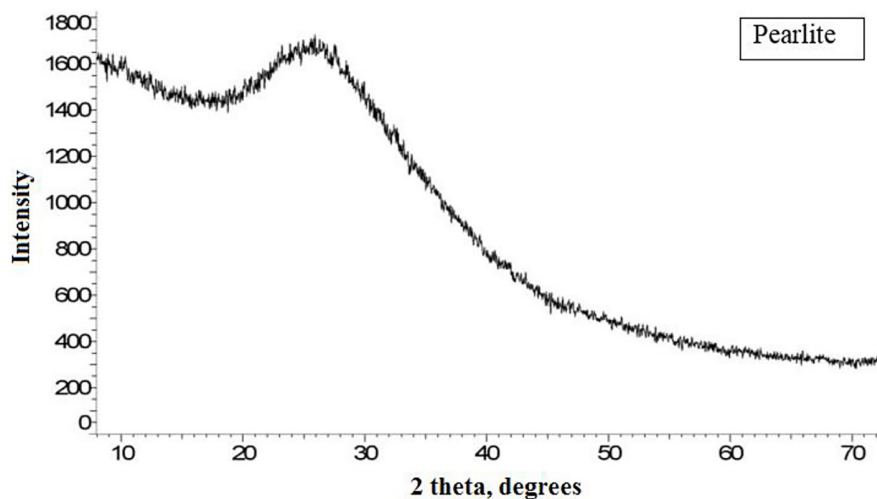


Figure 14. X-ray diffraction pattern for a sample made of expanded pearlite particles

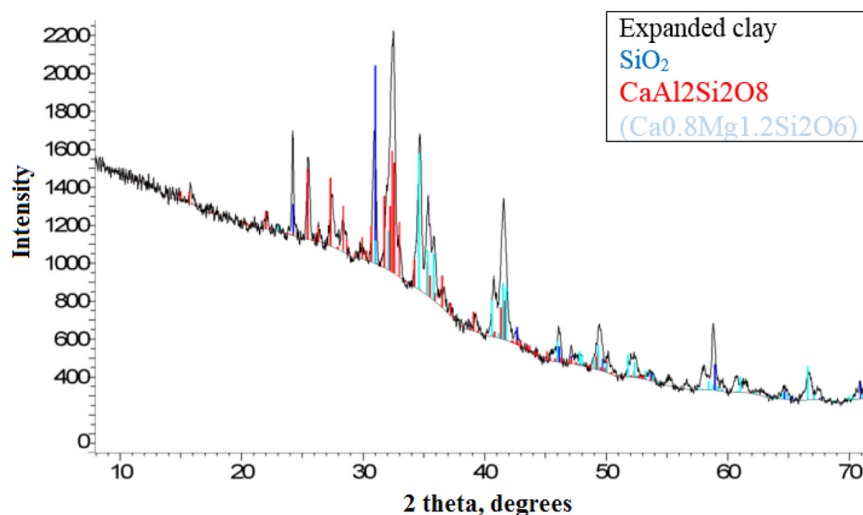


Figure 15. X-ray diffraction pattern for a sample made of expanded clay particles

to significant changes in the phase composition of the materials used. The same phases from which the component materials were composed were observed in the composite structure.

Figures 17 and 18 show diffractograms for AlSi12-Mg3/expanded perlite composites prepared with uncoated filler particles and with silicon-coated particles, respectively. Pearlite particles reacted with the aluminum alloy during the process. In the composite structure, both in the variant with uncoated filler particles and with coated particles, phases of the component materials were observed, and other complex phases were formed, i.e.  $(\text{FeMn})_3\text{Al}_2(\text{SiO}_4)_3$ ,  $\text{Al}_8\text{FeMg}_3\text{Si}_6$ . In the phase composition of AlSi12-Mg3/expanded clay composites (Figure 19 – variant with uncoated filler particles, Figure 20 – variant

with filler particles covered with silicon), phases originating from the composite materials were also observed, but the multi-component  $\text{Al}_8\text{FeMg}_3\text{Si}_6$  phase was also formed.

### Density measurements

Table 3 summarizes the results of density measurements for the component materials and the manufactured composites. Mineral filler particles (zeolite, expanded perlite, expanded clay) with a fraction of 4–6 mm are characterized by a much lower density compared to the AlSi12-Mg3 aluminum alloy. The use of these light particles made it possible to obtain composites with relatively low density. The lowest density was obtained when the filler was expanded perlite.

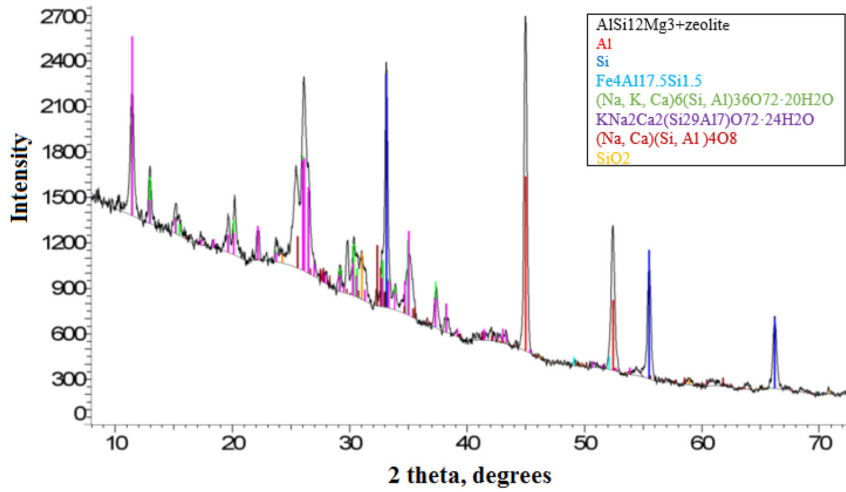


Figure 16. X-ray diffraction pattern for a sample of AlSi12-Mg3/zeolite composite with silicon-coated filler particles

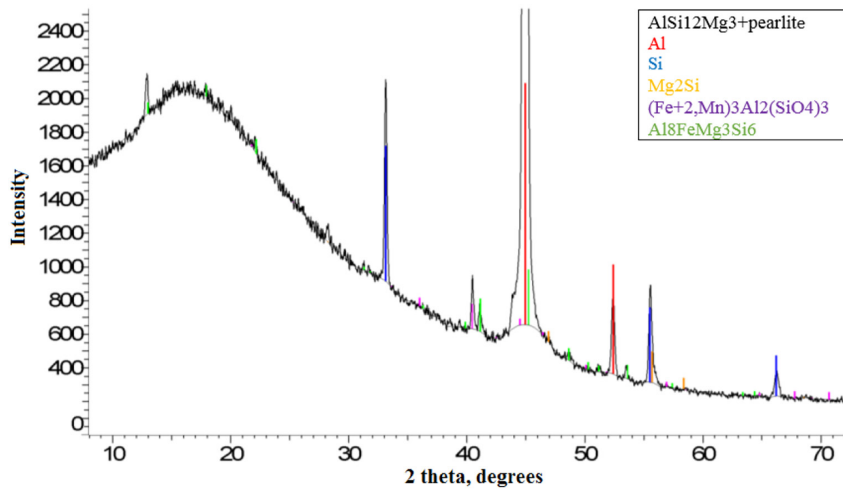


Figure 17. X-ray diffractogram for a sample of the AlSi12-Mg3/expanded perlite composite with uncoated filler particles

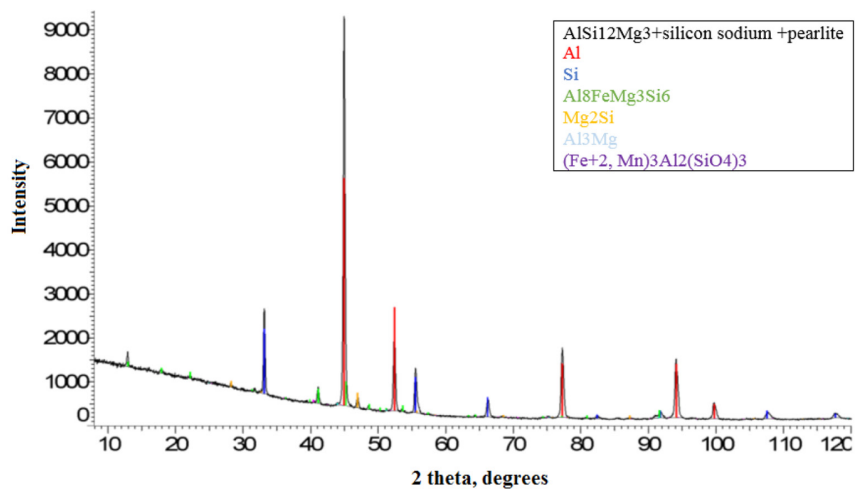


Figure 18. X-ray diffraction pattern for a sample of the AlSi12-Mg3/expanded perlite composite with silicon-coated filler particles

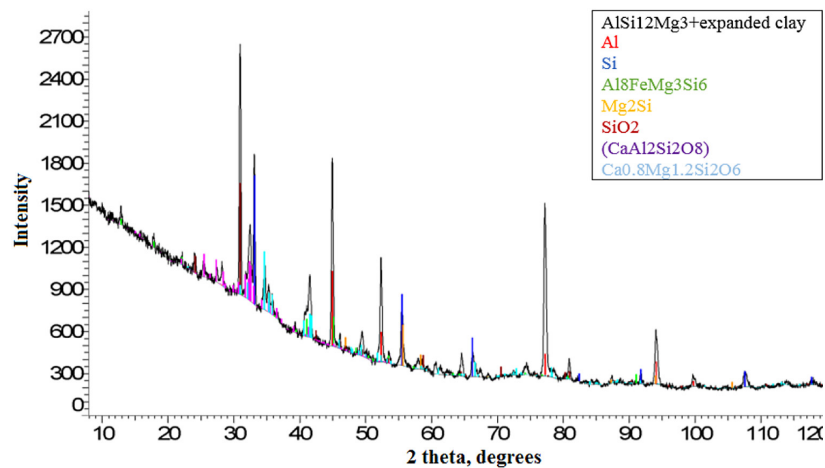


Figure 19. X-ray diffractogram pattern for a sample of the AlSi12-Mg3/expanded clay composite with uncoated filler particles

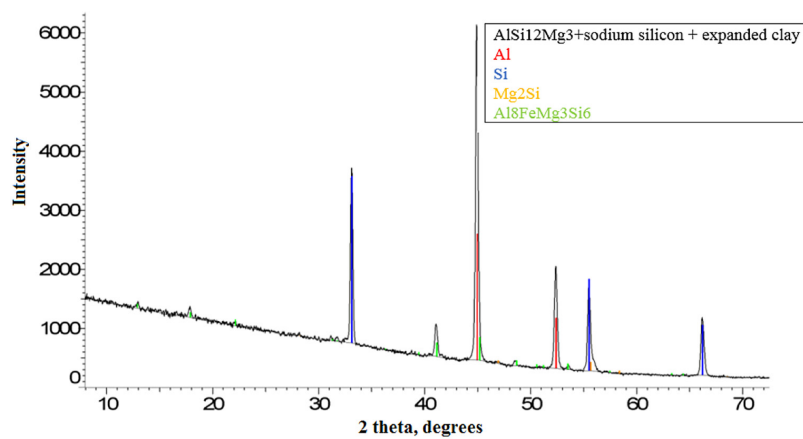


Figure 20. X-ray diffractogram for a sample of the AlSi12-Mg3/expanded clay composite with silicon-coated filler particles

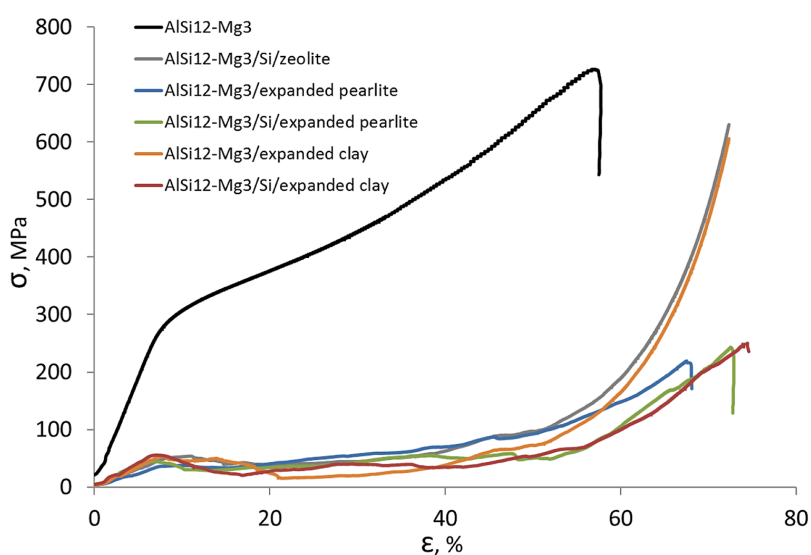
### Compressive strength measurements

Figure 21 shows representative compression test curves of the analyzed samples, presented in the form of engineering charts. Average values of the yield strength and compressive strength (measurements for at least 3 samples from the analyzed material) are summarized in Table 4. The yield strength for the AlSi12-Mg3 alloy was 240.1 MPa. Above this stress, the material deformed plastically until it reached the engineering failure stress of 746.3 MPa, which was accompanied by significant plastic deformation and an increase in the sample cross-section. In the case of compression tests of the produced composites, significantly lower values of the conventional yield strength were achieved (average values 39.1–50.6 MPa). After exceeding the yield point, the composite samples deformed without maintaining a constant

volume. The increasing deformation did not result in a proportional increase in the compressive cross-section. The obtained results show a large range of plastic deformation of the tested materials while maintaining a relatively constant value of compressive stress. Only with significant deformation (approximately 50–60%) was a clear increase in the engineering stress value observed, which may indicate significant deformation of the porous filler particles and reduction of their volume in the composite structure. During compression tests, no effect of covering the filler particles with silicon on the compressive strength of the tested composites was observed. The damage mechanism of Al-mineral particles composites is characterized by a layer-by-layer mode in which uniform and continuous deformation occurs. A similar phenomenon was observed by Orbulov [26] and Sanchez [27] in their research. No

**Table 3.** Results of density measurements

Material	Apparent density, $g/cm^3$	% of AlSi12-Mg3 alloy density
AlSi12-Mg3	2.60±0.01	100
Zeolite	1.83±0.03	70
Expanded pearlite	0.23±0.02	9
Expanded clay	0.48±0.06	18
AlSi12-Mg3/Si/zeolite	2.10±0.15	81
AlSi12-Mg3/expanded pearlite	1.33±0.08	51
AlSi12-Mg3/Si/expanded pearlite	1.32±0.07	51
AlSi12-Mg3/expanded clay	1.62±0.09	62
AlSi12-Mg3/Si/expanded clay	1.59±0.11	61



**Figure 21.** Representative engineering plots of shear tests for the AlSi12-Mg3 alloy sample and the analyzed composites

**Table 4.** Results of the compression test of the matrix material and the analyzed composites (values for engineering diagrams)

Material	Yield strength ( $R_{0.2}$ ), MPa	Compressive strength ( $R_C$ ), MPa
AlSi12-Mg3	240.1±24.4	746.3±31.4
AlSi12-Mg3/Si/zeolite	50.6±6.1	X
AlSi12-Mg3/expanded pearlite	39.1±3.0	X
AlSi12-Mg3/Si/expanded pearlite	41.0±3.7	X
AlSi12-Mg3/expanded clay	43.4±6.8	X
AlSi12-Mg3/Si/expanded clay	46.2±8.1	X

**Note:** x – measurement is not possible due to the lack of destruction of all samples of the analyzed material up to the maximum compressive force.

obvious shear bands were found at an angle of 45° with respect to the compression direction. Similar results were obtained in their studies by, among others, Movahedi and Majlinger, who used various filling particles [28, 29].

### CONCLUSIONS

The research has shown that it is possible to produce a composite based on aluminum alloys with a mineral filler with a porous structure using

gravity casting into sand molds. The obtained results of tests conducted in conditions similar to industrial ones enabled the selection of composite materials, which can be used to produce a composite characterized by low density and favorable functional properties. The selected component materials included casting aluminum alloy AlSi12-Mg3 (composite matrix material) and a mineral filler in the form of zeolite, expanded perlite or expanded clay with a particle diameter of 4–6 mm. Analyzes for various process parameters made it possible to determine the possibility of shaping the composite structure and, consequently, influencing its properties. From the performed investigations the following conclusions can be drawn.

In the case of a composite containing a filler in the form of zeolite particles, it was necessary to cover the filler with silicon powder by mixing it with an aqueous solution of sodium silicate (sodium water glass). The applied coating influenced the viscosity and surface phenomena of the liquid aluminum alloy in contact with the surface of the filler particles, resulting in an improvement in the possibility of the liquid Al alloy penetrating into the spaces between the filler particles. By using a filler in the form of expanded perlite or expanded clay, it was possible to create a composite with favorable structure and properties, both with uncoated filler particles as well as using a silicon-coated filler.

The results of structural and phase analyzes showed that the filler particles are evenly distributed against the background of the composite matrix, and during the manufacturing process, reactions may occur that result in the formation of new phases. Phase analysis and microscopic observations made it possible to obtain useful information on the impact of the component materials used and the parameters of the composite manufacturing process on the structure and phase composition of the product, which are directly related to the possibility of shaping the functional properties of the manufactured material. Fabricated composites were characterized by much lower density compared to aluminum alloys. The lowest density, 51% of the density of the Al12-Mg3 alloy, had composites containing an expanded perlite filler.

The produced materials were characterized by lower compressive strength compared to the Al-Si12-Mg3 alloy, however, the possibility of significant plastic deformation was observed. There was no effect of covering the filler particles with silicon on the compressive strength. Composites made using silicon-covered filler were characterized by

a yield strength similar to that of composites obtained using uncoated filler particles.

The low density of the fabricated composites, combined with their favorable structure and strength properties, suggest the possibility of use as light products transferring compressive stresses, as well as energy-absorbing products, such as: covers, controlled crumple zones, vibration dampers, energy absorbers, and other similar elements.

## REFERENCES

1. Maroti J. E., Orbulov I. N. Characteristics compressive properties of AlSi7Mg matrix syntactic foams reinforced by Al<sub>2</sub>O<sub>3</sub> or SiC particles in the matrix, *Mater. Sci. Eng. A.*, 2023, 869, 144817. <https://doi.org/10.1016/j.msea.2023.144817>.
2. Rajak D.K., Mahajan N.N., Linul E. Crashworthiness performance and microstructural characteristics of foam filled thin-walled tubes under diverse strain rate, *J. Alloys Compd.*, 2019, 775, 675–689. <https://doi.org/10.1016/J.JALLCOM.2018.10.160>.
3. Song J., Xu S., Xu L., Zhou J., Zou M. Experimental study on the crashworthiness of bio-inspired aluminum foam filled tubes under axial compression loading, *Thin-Walled Struct.*, 2020, 155, 106937. <https://doi.org/10.1016/j.tws.2020.106937>.
4. Alteneiji M., Krishnan K., Guan Z.W., Cantwell W.J., Zhao Y., Langdon G. Dynamic response of aluminum matrix syntactic foams subjected to high strain-rate loadings, *Compos. Struct.*, 2023, 303, 116289. <https://doi.org/10.1016/J.COMPSTRUCT.2022.116289>.
5. Thalmaier G., Sechel N.A., Csapai A., Popa C.O., Batin G., Gabora A. Aluminum perlite syntactic foams, *Materials*, 2022, 15, 5446. <https://doi.org/10.3390/ma15155446>.
6. Jung J., Kim S.H., Kang J.H., Park J., Kim W.K., Lim C.Y. Compressive strength modeling and validation of cenosphere-reinforced aluminum-magnesium matrix based syntactic foams, *Mater. Sci. Eng. A.*, 2022, 143452. <https://doi.org/10.1016/j.msea.2022.143452>.
7. Linul E., Lell D., Movahedi N., Codrean C., Fiedler T. Compressive properties of zinc syntactic foams at elevated temperatures, *Compos. B Eng.*, 2018, 167, 122–134. <https://doi.org/10.1016/j.compositesb.2018.12.019>.
8. Kemeny A., Katona B., Movahedi N., Fiedler T. Fatigue tests of zinc aluminum matrix syntactic foams filled with expanded pearlite, *IOP Conf. Ser. Mater. Sci. Eng.*, 2020, 903, 012050. DOI 10.1088/1757-899X/903/1/012050.
9. Castro G., Nutt S.R. Synthesis of syntactic steel foam using gravity-fed infiltration, *Mater. Sci. Ebg.*

- A., 2012, 553, 89–95. <https://doi.org/10.1016/j.msea.2012.05.097>.
10. Mandal D.P., Majumdar D.D., Bharti R.K., Majumdar J.D. Microstructural characterization and property evaluation of titanium cenosphere syntactic foam developed by powder metallurgy route. *Powder Metall.*, 2015, 58, 289–299. <https://doi.org/10.1179/1743290115Y.0000000012>.
  11. Pan L., Rao D., Yang Y., Qiu J., Sun J., Gupta N. Gravity casting of aluminum - Al<sub>2</sub>O<sub>3</sub> hollow sphere syntactic foams for improved compressive properties. *J. Porous Mater.*, 2020, 27, 1127–1137. <https://doi.org/10.1007/s10934-020-00889-x>.
  12. Anbuezhhiyan G., Mohan B., Sathianarayanan D., Muthuramalingam T. Synthesis and characterization of hollow glass microspheres reinforced magnesium alloy matrix syntactic foam. *J. Alloys Compd.*, 2017, 719, 125–132. <https://doi.org/10.1016/j.jallcom.2017.05.153>.
  13. Vendra L.J., Nexille B., Rabiei A. Fatigue in aluminum- steel and steel-steel composite foams. *Mater. Sci. Eng. A.*, 2009, 517, 146–153. <https://doi.org/10.1016/j.msea.2009.03.075>.
  14. Wiener C., Chmelik F., Ugi D., Mathis K., Knappek M. Damage characterization during compression in a perlite-aluminum syntactic foam. *Materials*, 2019, 12. <https://doi.org/10.3390/ma12203342>.
  15. Wright A., Kennedy A. The processing and properties of syntactic Al foams containing low cost expanded glass particles. *Adv. Eng. Mater.*, 2017, 19, 1–6. <https://doi.org/10.1002/adem.201600467>.
  16. Puga H., Carneiro V.H., Jesus C., Pereira J., Lopes V. Influence of particle diameter in mechanical performance of Al expanded clay syntactic foams. *Compos. Struct.*, 2018, 184, 698–703. <https://doi.org/10.1016/j.compstruct.2017.10.040>.
  17. Su M., Wang H., Hao H. Compressive properties of aluminum matrix syntactic foams prepared by stir casting method. *Adv. Eng. Mater.*, 2019, 1900183. <https://doi.org/10.1002/adem.201900183>.
  18. Huang W., Liu G., Li H., Wang F., Jurczyk M. Compressive properties and failure mechanisms of gradient aluminum foams prepared by a powder metallurgy method. *Metals.*, 2021, 11(9), 1337. <https://doi.org/10.3390/met11091337>.
  19. Sahu S., Ansari M.Z., Mondal D.P., Cho C. Quasi-static behavior of aluminum cenosphere syntactic foams. *Mater. Sci. Technol.*, 2019, 35, 7. <https://doi.org/10.1080/02670836.2019.1593670>.
  20. Qu H., Rao D., Cui J., Gupta N., Wang H., Chen Y., Li A., Pan. L. Mg-matrix syntactic foam filled with alumina hollow spheres coated by MgO synthesized with solution coating- sintering. *J. Mater. Res. Technol.*, 2023, 24, 2357–2371. <https://doi.org/10.1016/j.jmrt.2023.03.160>.
  21. Władysław R., Kozuń A., Dębowska K., Pacyniak T. Analysis of crystallization process of intensive cooled AlSi20CuNiCoMg. *Arch. Foundry Eng.*, 2017, 2, 137–144. <https://doi.org/10.1515/afe-2017-0065>.
  22. Borowiecka- Jamorezk J., Kargul M. Effect of zeolite addition on the production of a cast porous composite based on AC-AlSi11 silumin. *Arch. Foundry Eng.*, 2022, 4, 96–101. [10.24425/afe.2022.143956](https://doi.org/10.24425/afe.2022.143956).
  23. Taherishargh M., Linul E., Broxtermann S., Fiedler T. The mechanical properties of expanded perlite-aluminum syntactic foam at elevated temperatures. *J. Alloys Compd.*, 2018, 737, 590–596. <https://doi.org/10.1016/j.jallcom.2017.12.083>.
  24. Kemeny A., Leveles B., Karoly D. Functional aluminum matrix syntactic foams filled with lightweight expanded clay aggregate particles. *Mater. Today Proc.*, 2021, 45, 4229–4232. <https://doi.org/10.1016/j.matpr.2020.12.164>.
  25. Qu H., Rao D., Cui J., Gupta N., Wang H., Chen Y., Pan. L. Mg alloy syntactic foams filled with MgO coated Al<sub>2</sub>O<sub>3</sub> hollow spheres: microstructure and mechanical properties. *Res Sq.*, 2022, <https://dx.doi.org/10.2139/ssrn.4229761>
  26. Orbulov I.N., Szlancsik A., Kemeny A., Kincses D. Low-cost light-weight composite metal foams for transportation applications, *J. of Materi Eng and Perform*, 2022, 6954–6961. <https://doi.org/10.1007/s11665-022-06644-4>
  27. Sánchez de la Muela, A.M., García Cambronero, L.E., Malheiros, L.F., Ruiz-Román, J.M. New Aluminum Syntactic Foam: Synthesis and Mechanical Characterization, *Materials*, 2022, 15, 5320. <https://doi.org/10.3390/ma15155320>.
  28. Movahedi N., Murch G.E., Belova I.V., Fiedler T. Functionally graded metal syntactic foam: fabrication and mechanical properties, *Mater. Des.*, 2019, 168, 107652. <https://doi.org/10.1016/j.matdes.2019.107652>.
  29. Majlinger K., Orbulov I.N. Characteristic compressive properties of hybrid metal matrix syntactic foams, *Mater. Sci. Eng. A.*, 2014, 606, 248–256. <https://doi.org/10.1016/j.msea.2014.03.100>.